

Linköping University Post Print

Fullerene-like CS_x: A first-principles study of synthetic growth

Cecilia Goyenola, Gueorgui Kostov Gueorguiev, Sven Stafström and Lars Hultman

N.B.: When citing this work, cite the original article.

Original Publication:

Cecilia Goyenola, Gueorgui Kostov Gueorguiev, Sven Stafström and Lars Hultman, Fullerene-like CS_x: A first-principles study of synthetic growth, 2011, CHEMICAL PHYSICS LETTERS, (506), 1-3, 86-91.

<http://dx.doi.org/10.1016/j.cplett.2011.02.059>

Copyright: Elsevier Science B.V., Amsterdam.

<http://www.elsevier.com/>

Postprint available at: Linköping University Electronic Press

<http://urn.kb.se/resolve?urn=urn:nbn:se:liu:diva-67563>

Fullerene-like CS_x : A first-principles study of synthetic growth

C. Goyenola, G. K. Gueorguiev, S. Stafström, L. Hultman

*Department of Physics, Chemistry and Biology (IFM), Linköping University, SE 581-83,
Linköping, Sweden*

ABSTRACT

Fullerene-Like (FL) sulpho-carbide (CS_x) compounds have been addressed by first principles calculations. Geometry optimization and cohesive energy results are presented for the relative stability of precursor species such as C_2S , CS_2 , and C_2S_2 in isolated form. The energy cost for structural defects, arising from the substitution of C by S is also reported. Similar to previously synthesized FL- CN_x and FL- CP_x compounds, the pentagon, the double pentagon defects as well as the Stone-Wales defects are confirmed as energetically feasible in CS_x compounds.

1. INTRODUCTION

Carbon based fullerene-like (FL) compounds have been developed as a new class of materials exhibiting outstanding mechanical properties such as compliance, low plasticity and mechanical resilience [1, 2] as in carbon nitride (CN_x) [1, 3, 4] and phosphorus carbide (CP_x) [2, 5, 6, 7] thin films. Substitution of carbon atoms by N or P atoms promotes bending in the graphene network by pentagon formation, as well as cross-linkage between graphene planes. The bending and cross-linking of the graphene planes

extends the strength of a planar sp^2 coordinated network in three dimensions. The deposition method of choice for these compounds is reactive magnetron sputtering. During deposition, precursors C_mX_n ($X = N, P, S.$) are formed in the deposition chamber and they are attached to the edge of the growing film, thus playing an important role in the formation of the film structure.

The Synthetic Growth Concept (SGC) based on the Density Functional Theory [4, 6, 8, 9] for simulations of film formation during vapor phase deposition was developed by this group. SGC treats structural evolution by sequential steps of atomic rearrangement where each step is assigned according to the previous relaxed states. Specifically, the properties of precursors for nanostructured compounds are described quantitatively together with their interaction with the film edge during formation of condensed phases.

In this work, sulfur is addressed as a prospective dopant for the synthesis of a new FL solid compound – the FL sulpho-carbide (FL- CS_x). Thus, the aim is to enlarge the class of thin solid films with FL properties, by adopting another dopant element belonging to the sub-matrix of the periodic table containing the p-elements.

Recent *ab initio* studies carried out by others show that, similar to what happens in CN_x and CP_x [4, 6, 8], doping graphene layers with S promotes bending of the graphene planes [10, 11] which is perceived as favorable regarding the possibility for future synthesis of FL- CS_x . However, there were no systematic attempts to address solid CS_x in the context of deposition of this compound, as understood in SGC [4, 6, 8].

The scope of this work is to address the stability of the C_mS_n precursor species that are

expected to belong to the growth flux during vapor phase deposition of FL-CS_x thin films. The generic and structure-defining defects in FL-CS_x are also evaluated by considering CS_x model systems in which C atoms are substituted by S atoms in an sp²-hybridized finite graphene-like network. The study involves both geometry optimizations and cohesive energy calculations performed within the framework of SGC. This approach was successfully applied to FL-CN_x [4, 8] and FL-CP_x [5, 6]. The preformed species *SCS*, *CCS*, *C₂S^t* (“t”: triangular shape of the molecule) and *SCCS* (configurational formulas for these precursors are adopted here in order to distinguish the atomic sequences in the species), as well as some of the pure S clusters such as the *S₃* and *S₄* chains, were all found to be among the most stable precursors in the FL-CS_x growth environment.

Regarding the typical defects occurring in FL-CS_x, the Stone-Wales defects, together with different combination of pentagon defects emerge as likely defect patterns in FL-CS_x. Taking into account the selection of defects for CS_x, the graphene layers in FL-CS_x are expected to be more curved than in FL-CN_x, but due to unlikeliness of tetragonal defects in CS_x, to exhibit less curvature than in FL-CP_x.

2. COMPUTATIONAL DETAILS

The framework adopted for the present calculations is Density Functional Theory (DFT) within its generalized gradient approximation (GGA) as implemented in the *Gaussian 03 code* [12].

A systematic study of film-forming *C_mS_n* ($m \leq 2$, $n \leq 4$) and *S_n* ($n \leq 4$, $n = 8$) species was carried out by geometry optimizations of different possible geometries of these small

clusters, radicals, and molecules. The energy cost for substitutional S at C sites in graphene layers was investigated by geometry optimizations covering a wide diversity of defects resulting from the S incorporation.

The cohesive energy per atom ($E_{coh/at}$) was calculated for the systems of interest, understanding the cohesive energy as the energy that is necessary to break the system into isolated atoms. $E_{coh/at}$ is defined in equation 1 as the total energy of model system minus the energy of each individual atom, divided by the total number of sulfur and carbon atoms:

$$E_{coh/at} = \left| \frac{E_{system} - N_H \times E_H - N_C \times E_C - N_S \times E_S}{N_C + N_S} \right|, \quad (1)$$

where N_H , N_C and N_S are the number of hydrogen, carbon and sulfur atoms, respectively; and E_H , E_C , and E_S are the total energy of the corresponding free atoms in ground state.

Concerning the DFT–GGA level of theory, both the Perdew–Wang exchange–correlation functional (PW91) [13] and the B3LYP hybrid functional [14] were used. Both functionals are known to provide an accurate description of the structural and electronic properties of FL thin films [6, 8] and similar covalent systems [15, 16, 17]. The results reported in this work were obtained using the PW91 exchange correlation functional (making use of the 6-31G** basis set augmented with polarization functions), while the B3LYP simulations were carried out for comparative purposes. **In order to ensure that the anions are properly described, selected precursors were addressed by test calculations**

employing a basis set including diffuse functions (6-31++G**).

3. RESULTS AND DISCUSSION

3.1. Precursors

The systematic study of the precursors comprised a variety of different possible conformations for the C_mS_n molecules and radicals. Their choice takes into account:

- (i) The chemistry of the sulfur when interacting with carbon [18];
- (ii) The specific aim to address the FL- CS_x from point of view of thin film growth by magnetron sputtering as well as previous experience with FL- CN_x and FL- CP_x films. (e.g., similarly to CN_x and CP_x , sulfur concentration of interest is perceived as being below 30 at.% in a realistic sputtering target, in the deposition environment as well as in the films; only small precursors consisting of not more than several atoms are considered, etc.).

The following precursors were considered C_2 , CS , S_2 , C_2S , CS_2 , C_2S_2 , C_3S , C_2S_4 , as well as, pure sulfur clusters containing 3, 4 and 8 atoms (S_8 was taken as a reference representing a well known stable and symmetric pure sulfur cluster and not as a prospective CS_x precursor). In total, 41 plausible candidate conformations of the above mentioned species were submitted to geometry optimization and described by structural parameters and cohesive energy per atom. In order to test the feasibility of the corresponding energy minima the Vibrational spectra of relaxed structures were calculated. 17 species were selected as prospective precursors, the selection criteria being:

- (i) Relative stability;
- (ii) Similarity to known molecules and radicals;
- (iii) Existing theoretical and experimental knowledge for precursors relevant to FL-CN_x and FL-CP_x compound deposited by magnetron sputtering [2, 4, 5].

The selected precursors were considered both as neutral and as anionic species. Fig. 1 and Fig. 2 show the corresponding optimized precursors. “Bonds” are indicated at the figures only for those inter-atomic distances that do not differ more than 15% from an average experimentally known distance found in sulfur-organic compounds (namely, for C-S bonds this average experimental value is 1.78 Å, for C-C bonds - 1.37 Å, and for S-S bonds 1.98 Å) [19-23].

3.1.1. C_mS_n

The bond lengths and cohesive energies obtained for both neutral and anion dimers C_2 , CS , and S_2 are listed in Table 1. Their relative stability is as follows in order of decreasing E_{coh} : for neutrals CS , C_2 , S_2 ; and for anions C_2^{-1} , CS^{-1} , S_2^{-1} . Calculated bond lengths for the neutral CS and S_2 are within 3% of bond lengths experimentally obtained for these species in gas phase [19]. The relation in bond lengths, in order of increasing bond lengths, is C_2 , CS , S_2 for both neutrals and anions, which is in agreement with Ref. 19.

The relaxed neutral and anion trimers C_2S and CS_2 are displayed in Fig. 1a. The corresponding cohesive energies per atom are listed in Table 2.

In the case of CS_2 , a variety of geometries were considered with the following outcome:

- (i) Linear structures, with atom sequences SCS and SSC , from which SCS displays increased stability of 6.17 eV/at;
- (ii) A triangular structure CS_2^t (Fig. 1a) is found to be another stable CS_2 conformation (5.24 eV/at).

Considering the corresponding anions, the SCS anion specie is less stable compared to the neutral; this is expected since the neutral species is the stable carbon disulfide molecule. The bond length obtained for the relaxed SCS species agrees with the value of 1.55 Å reported for the well known CS_2 molecule in the gas phase [19].

For C_2S , both triangular (C_2S^t) and linear conformations (CCS , CSC) were considered, the triangular being energetically favored. For these species, the cohesive energy is higher for the neutral counterparts (Table 2). For CCS and C_2S^t anionic species, due to charge redistribution, the S-C bonds stretch while C-C bonds contract (Fig. 1a).

Two tetramers were studied: C_2S_2 and C_3S . No stable structure was found for C_3S . $E_{\text{coh/at}}$ for the relaxed C_2S_2 conformations are listed in Table 2 and the optimized structures are displayed in Fig. 1b. In the case of the tetrahedron (Fig. 1b, C_2S_2), both anion and neutral species easily dissociate into C_2 and S_2 dimers. Again, as in the case of the trimers, adding an electron to the linear structure $CSCS$ to obtain an anion, leads to contraction of the C-C bond and stretching of the S-C bond length.

The geometry preferred for C_2S_4 (which can be seen as composed by two trimers CS_2) is

not only stable, but this conformation is also a well-known common building block of sulfur-containing organic molecules [23]. In agreement with the results obtained by Maeyama *et al.*, [24] and Wen Zhang *et al.* [25], the relaxed geometry of this cluster is slightly distorted (the bond lengths differing by 5% approximately from their values if the cluster retains perfect symmetry).

3.1.2. S_n ($n=3,4,8$)

The relaxed conformations for S_3 are found to be a triangle and a chain. For S_4 , a square shape and a chain were obtained. In the case of S_8 molecule - the emblematic ring structure, which is the building block of one of the allotropic forms of sulfur [19], was studied.

A comprehensive graph of $E_{\text{coh/at}}$ as a function of the number of atoms in S_n clusters is shown in Fig. 2 together with the corresponding conformation of the most stable species. The dimers S_2 and C_2 are included in the graph for comparative purposes. As seen from Fig. 2, for S_3 and S_4 , the chain conformations represent stability advantages compared to their ring counterparts. $E_{\text{coh/at}}$ data for the relaxed chain-like species is listed in Table 3. For S_3 (chain), the S-S bond length is 1.96 Å and the bond angle is 118.9°. In the case of S_4 , the S-S bond lengths are 1.95 Å for the external bond and 2.19 Å for the internal bond; the bond angle is 111.5° (see Fig. 2). When excited, the S_4 cluster dissociates easily into 2 dimers. Both S_3 and S_4 anions exhibit increased stability in comparison to their neutral counterparts (Table 3). Similar structural features of small pure sulfur clusters were found by others at the same level of theory. [26-28]

The stable S_8 conformation exhibits a crown-like shape (Fig. 2). For this shape, all bond lengths (2.10 Å) and all bond angles (109.7°) are the same within the error margin. These results agree well with the structural features obtained experimentally for S_8 in gas phase (bond length of 2.07 Å and bond angle of 105°) [19]. As expected, the S_8 anion undergoes a distortion becoming susceptible to dissociation when structurally perturbed.

Addressing both neutral and anionic species and taking into account their dissociation under excitation permits an efficient selection of the precursors which are active during FL- CS_x deposition by magnetron sputtering.

3.2. Defects in the CS_x network

By considering graphene-like model systems, the following structural defects in a sulfur doped graphene network were addressed:

- (i) Pentagon defect (including single (SPent) and double (DPent) pentagon defect), Fig. 3a, and 3b, respectively;
- (ii) Stone – Wales defect (SW), Fig. 3c;
- (iii) Tetragon defect (Tetr), Fig. 3d.

A pure hexagonal carbon structure without defects (Hex), Fig. 3e, was also simulated for reference purposes. All possible S substitutions at C sites (with the exception of the case of the SW defect for which too many permutations of S sites are possible) were considered. Different S substitution sites are marked with numbers in Fig. 3. Successful relaxation for all model systems considered here indicates that different S-containing

defects are stable and can prevail in a CS_x network. Stoichiometries for the model systems are listed in Table 4. Only the S-substituted defects in position 1 (which is always an internal and not peripheral site for each model system, thus avoiding boundary effects) are listed in Table 4, while their corresponding optimized structures are displayed in Fig. 4. In order to ensure that the energy cost results do not depend on the size and shape of the model systems chosen, most of the calculations were repeated for larger model systems incorporating the same defects. No significant differences in the energy costs were found.

In the case of the single pentagon defect (Fig. 4a), which is a typical defect in all FL solid compounds and an important structural feature inducing curvature to the graphene planes, the S-C bond length values are between 1.73 and 1.86 Å. The S-containing double pentagon defect exhibits similar variation of C-S bond lengths: 1.72 - 1.85 Å. Similar, (but to a lesser extent) to what happens in FL- CP_x compounds, in which P-atom at a C-site induces a local curvature, in CS_x the S atom at a C-site induces a local curvature and sticks out of this site original position in a pure graphene network (see Fig. 4b).

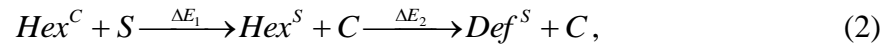
Concerning the tetragon defect (Fig. 4c), the calculated C-S bond length values vary considerably between 1.75 Å and 2.01 Å [20]. These should be compared to 1.77 Å and 2.04 Å for the CP_x analogue of this model system representing the tetragon defect [2].

The simulation results regarding the Stone-Wales defect indicate that when the S atom is in an inner position (positions 1-6 in Fig. 3c) the system expectedly adopts a curved

shape and the S atom sticks out of the system plane exhibiting S-C bond lengths in the range of 1.70 - 1.88 Å, Fig. 4d. When the S atom is at an external position (positions 7, 8 in Fig. 3c) of the model system, again expectedly remains to a large extent undistorted.

In the model systems designed to address the defects energetics in CS_x , the C-S bond length is in the range 1.70 - 1.90 Å (a smaller range of 1.70 - 1.81 Å was obtained for a strictly hexagonal CS_x network) while the range of the C-C bonds is 1.36 - 1.46 Å. These results agree well with the bond lengths data for a broad range of carbon and sulfur containing structures from the C_mS_n species considered in this work to the sulpho-organic compounds studied by others [10, 11].

In order to evaluate the cost of the S-containing ring defects, the following sequence of structural changes is perceived:



where “ Hex^C ” and “ Hex^S ” represent a pure graphene network and a graphene network with one C atom substituted by an S atom, “ Def^S ” represents the subsequent ring S-containing defect (e.g., a pentagon, SW defects, etc.). The cost for the formation of an S-containing ring defect starting from a pure graphene network is ΔE_T , defined as in equation 3.

$$\Delta E_T = \Delta E_1 + \Delta E_2, \quad (3)$$

where ΔE_1 , ΔE_2 express the changes in the cohesive energy per atom required for each of

the structural transformations described, defined as follows:

$$\Delta E_1 = E_{Hex^S+C} - E_{Hex^C+S} \quad (4)$$

$$\Delta E_2 = E_{Def^S+C} - E_{Hex^S+C} \quad (5)$$

It is trivial that single S and C atoms have 0 eV of cohesive energy and that these single atoms are included on the above indices for correctness of the chemical equations only. Actually, since for every act of defect creation ΔE_1 is a constant of 0.38 eV/at, the actual cost for a given S-containing defect is determined by ΔE_2 . Table 5 lists the energy costs ΔE_1 , ΔE_2 and the total energy cost ΔE_T in order of increasing ΔE_T . The single pentagon defect is the most energetically favorable defect ($\Delta E_T = 0.53$ eV/at), followed by the Stone – Wales defect by a difference of 0.02 eV/at (i.e., $\Delta E_T = 0.55$ eV/at) and by the double pentagon defect ($\Delta E_T = 0.64$ eV/at). The tetragon defect emerges as considerably more costly at $\Delta E_T = 0.82$ eV/at and consequently as not particularly likely in FL-CS_x.

For comparative purposes, the energy costs for the same types of defects as addressed here for CS_x, but occurring in FL-CN_x [4] and FL-CP_x [6] compounds are listed in the two columns at the right side of the Table 5. The comparison of the energy costs for typical defects in different FL compounds reveals that FL-CS_x exhibits an intermediate (but closer to FL-CP_x) situation between FL-CN_x and FL-CP_x with respect to likeliness of different types of defects. Single and double pentagon defects in FL-CS_x exhibit a similar energy cost as in FL-CP_x while the SW defect in FL-CS_x has the advantage of exhibiting nearly the same cost as the SPent in the same compound. The SW defect in FL-CS_x is

0.12 eV/at less costly than the same defect in FL-CP_x and by 0.14 eV/at more costly than in FL-CN_x. Considerable difference between FL-CS_x and FL-CP_x emerges with respect to the tetragon defect. Its energy cost in FL-CS_x of $\Delta E_T = 0.82$ eV/at is equal to the cost for the same defect in FL-CN_x and by 0.17 eV/at higher than the energy cost for the same defect in FL-CP_x where it plays a very important structural role. Since the average cost of typical defects in FL-CS_x is higher than the average cost of the same defects in FL-CN_x, while the energy cost of 0.82 eV/at excludes the tetragon defect from the range of structure defining defects in FL-CN_x, the same energy cost still leaves probabilities for this defect occurring in FL-CS_x. However, in contrast to the case of FL-CP_x the tetragon defect (and consequently cage-like formations seeded by a tetragon defect [6]) is not expected to be of significance during synthetic growth of FL-CS_x.

4. CONCLUSIONS

The precursors with more impact for synthetic growth of FL-CS_x by magnetron sputtering are, in order of decreasing stability, the neutral species SCCS, SCS, CCS, C₂S₄, CS, C₂S, C₂S₂, CSCS, CS₂, CSC, SSC, C₂, S₄, S₃, S₂; and the anions CCS, C₂S, C₂, CS₂, CS, and S₂.

The pentagon and double pentagon defects are quite stable in CS_x together with the Stone-Wales defect (energy costs of 0.53 eV/at, 0.64 eV/at, and 0.55 eV/at, respectively). This is due to the S atom expanding its d-orbitals as in, e.g., SF₆, thus stabilizing curved S-doped pentagon-containing graphene-like planes. On the other hand, the tetragon defects, theoretically predicted and experimentally confirmed as structure defining in FL-

CP_x , exhibit a considerably higher energy cost in FL- CS_x (0.82 eV/at as compared to 0.65 eV/at for FL- CP_x), so they are not expected to play an important role. They may, however, coexist with a variety of pentagon types of defects and Stone-Wales defects. This selection of prevailing defects in FL- CS_x places this compound in an intermediate position between FL- CN_x and FL- CP_x , i.e., graphene-like sheets are expected to be considerably shorter and more buckled than in FL- CN_x , but still less curved and interlocked than in FL- CP_x . Thus, FL- CS_x film may be possible to synthesize with a longer range order (less amorphous) than FL- CP_x .

5. ACKNOWLEDGMENTS

This research is supported by the Functional Nanoscale Materials (FunMat), VINN Excellence Center financed by the Swedish Governmental Agency for Innovation Systems (VINNOVA). G.K.G. gratefully acknowledges the Swedish Research Council (VR). The National Supercomputer Center in Linköping is acknowledged for providing high performance computing resources.

6. REFERENCES

- [1] L. Hultman, J. Neidhardt, N. Hellgren, H. Sjöström, J-E. Sundgren, MRS Bull. 28 (2003) 194-202.
- [2] A. Furlan, “*Fullerene-like CN_x and CP_x Thin Films; Synthesis, Modeling, and Applications*”. [Thesis]. Linköping: Linköping University Electronic Press; 2009.

Linköping Studies in Science and Technology. Dissertations, 1247.

[3] H. Sjöström, S. Stafström, M. Boman, J-E. Sundgren, Phys. Rev. Lett. Vol. 75, Num. 7 (1995) 1336-1339.

[4] G.K. Gueorguiev, J. Neidhardt, S. Stafström, L. Hultman, Chem. Phys. Lett. 410 (2005) 228.

[5] A. Furlan, G.K. Gueorguiev, H. Högberg, S. Stafström, L. Hultman, Thin Solid Films, 515 (2006) 1028-1032.

[6] G.K. Gueorguiev, A. Furlan, H. Högberg, S. Stafström, L. Hultman, Chem. Phys. Lett. 426 (2006) 374-379.

[7] F. Claeysens, G.M. Fuge, N.L. Allan, P.W. May, S.R.J. Pearce, M.N.R. Ashfold, Appl. Phys. A 79 (2004) 1237.

[8] G.K. Gueorguiev, J. Neidhardt, S. Stafström, L. Hultman, Chem. Phys. Lett. 401 (2005) 288.

[9] G.K. Gueorguiev, E. Broitman, A. Furlan, S. Stafström, L. Hultman, Chem. Phys. Lett. 482 (2009) 110.

[10] P.A. Dennis, R. Faccio, A.W. Mombrú, Chem. Phys. Chem. 10 (2009) 715-722.

[11] A.L.E. García, S.E. Baltazar, A.H. Romero, J.F. Pérez Robles, A. Rubio, J. Comput. Theor. Vol. 5, Num. 11 (2008) 1-9.

- [12] M.J. Frisch et al., Gaussian 03, Revision C.02, Gaussian, Inc., Wallingford, CT, 2004.
- [13] J. P. Perdew, J. A. Chevary, S. H. Vosko, K. A. Jackson, M. R. Pederson, D. J. Singh, and C. Fiolhais, Phys. Rev. B 46 (1992) 6671.
- [14] A. D. Becke, J. Chem. Phys. 98 (1993) 5648.
- [15] S. Stafström, L. Hultman, N. Hellgren, Chem. Phys. Lett. 340 (2001) 227.
- [16] R.-H. Xie, G.W. Bryant, L. Jensen, J. Zhao, V.H. Smith Jr., J. Chem. Phys. 118 (2003) 8621.
- [17] R.-H. Xie, G.W. Bryant, V.H. Smith Jr., Chem. Phys. Lett. 368 (2003) 486.
- [18] Shigeru Oae, "Organic Sulfur Chemistry: Structure and mechanism", CRC Press, 1st Ed. (1991).
- [19] "CRC Handbook of Chemistry and Physics" CRC Press, 91st Ed. (2010).
- [20] A.C. Gallacher, A.A. Pinkerton, Acta Crystallographica C, 49 (1993) 125-126.
- [21] N.C. Baenziger, W.L. Duax, J. Chem. Phys. 48 (1968) 2974-2981.
- [22] J. Steidel, R. Steudel, A. Kutoglu, Zeitschrift fuer Anorganische und Allgemeine Chemie, 476 (1981) 171-178.
- [23] V.N. Baumer, B.A. Starodub, V.P. Batulin, E.E. Lakin, V.P. Kuznetsov, O.A. D'yachenko, Acta Crystallographica C 49 (1993) 2051-2053.

- [24] T. Maeyama, T. Oikawa, T. Tsamura, N. Mikami, J. Chem. Phys. Vol. 108, Num. 4 (1998) 1368-1376.
- [25] S. Wen Zhang, C. Gang Zhang, Y. Tao Yu, Bing Zhi Mao, Fu Chu He, Chem. Phys. Lett. 304 (1999) 265-270.
- [26] R.O. Jones, P. Ballone, J. Chem. Phys. Vol. 118, Num. 20 (2003) 9257-9265.
- [27] K. Raghavachari, C. McMichael Rohifing, J.S. Binkley, J. Chem. Phys. Vol. 93, Num. 8 (1990) 5862-5874.
- [28] S. Hunsicker, R. O. Jones, G.Ganteför, J. Chem. Phys. Vol. 102, Num. 15 (1995) 5917-5936.

TABLE CAPTIONS

Table 1. Bond lengths and cohesive energies for dimers C_2 , CS , and S_2 .

Table 2. Cohesive energies per atom for trimers (C_2S and CS_2), tetramers (C_2S_2), and C_2S_4 .

Table 3. Cohesive energies per atom for pure sulfur precursors.

Table 4. Stoichiometry for the pure carbon structures of interest: cohesive energies per atom for model systems with a substitution S atom in position 1.

Table 5. Cost of the S-substitution in C-sites for the model systems displayed in Fig. 3 (S atom at position 1). For comparison, the energy costs for the same types of defects in FL- CN_x [4] and FL- CP_x [6] compounds are listed in the two columns two the right. The arrow indicates the direction of increasing energy costs for S-containing ring defects.

TABLES

Table 1.

Dimer	Bond Length (Å)		Cohesive Energy (eV/at)	
	Neutral	Anion	Neutral	Anion
C ₂	1.41	1.33	4.39	6.31
CS	1.56	1.69	5.73	5.51
S ₂	1.94	2.05	3.64	4.82

Table 2.

Structure	<i>SCS</i>	<i>SSC</i>	<i>CS₂^t</i>	<i>CSC</i>	<i>CCS</i>	<i>C₂S^t</i>	<i>CSCS</i>	<i>SCCS</i>	<i>C₂S₂</i>	<i>C₂S₄</i>	
E _{Coh} (eV/at)	Neutral	6.17	4.68	5.24	4.96	6.21	5.77	5.37	6.52	5.54	5.97
	Anion	6.07	-	6.18	5.45	6.91	6.48	5.81	7.00	6.01	6.36

Table 3.

Structure	<i>S₃</i>	<i>S₄</i>	<i>S₈</i>	
E _{coh} (eV/at)	Neutral	4.25	4.31	4.49
	Anion	5.02	4.96	-

Table 4.

Name	Stoichiometry	<i>E_{coh/at}</i> (eV/at)
(a) Tetr	<i>C₁₆H₈</i>	10.30
(b) DPent	<i>C₁₄H₈</i>	10.47
(c) SPent	<i>C₂₀H₁₀</i>	10.58
(d) Hex	<i>C₂₄H₁₂</i>	10.73
(e) SW	<i>C₄₂H₁₆</i>	10.56

Table 5

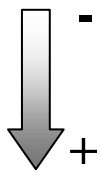
Structure	ΔE_1 (eV/at)	ΔE_2 (eV/at)	ΔE_T (eV/at)		FL-CN _x ΔE_T (eV/at)	FL-CP _x ΔE_T (eV/at)
Hex	0.38	0.00	0.38		0.11	0.41
SPent	0.38	0.15	0.53		0.30	0.52
SW	0.38	0.17	0.55		0.41	0.63
DPent	0.38	0.27	0.64		0.26	0.56
Tetr	0.38	0.44	0.82		0.82	0.65

FIGURE CAPTIONS

Figure 1. Optimized structures for neutral C_mS_n precursors, (a) trimers, (b) tetramer species, and the C_2S_4 molecule. Bond lengths are in Å and bond angles are in degrees. The values between parentheses correspond to the optimized structure of the anion species.

Figure 2. $E_{\text{coh/at}}$ as a function of number of S atoms for pure sulfur species (C_2 is included as a bench mark), the graph points are represented by asterisks.

Figure 3. Model systems representing: (a) single pentagon defect (SPent); (b) double pentagon defect (DPent); (c) Stone – Wales defect (SW); (d) tetragon defect (Tetr); (e) pure hexagonal network (Hex). Numbers indicate the different positions for the S-atom which were considered during optimizations.

Figure 4. Defect containing model systems (from Fig. 3) after relaxation: (a) SPent1; (b) DPent1; (c) Tetr1; (d) SW1, front view; (e) SW1, side view; (f) Hex1. The number “1” after the defect abbreviation indicates the position of the S atom within the model system.

FIGURES

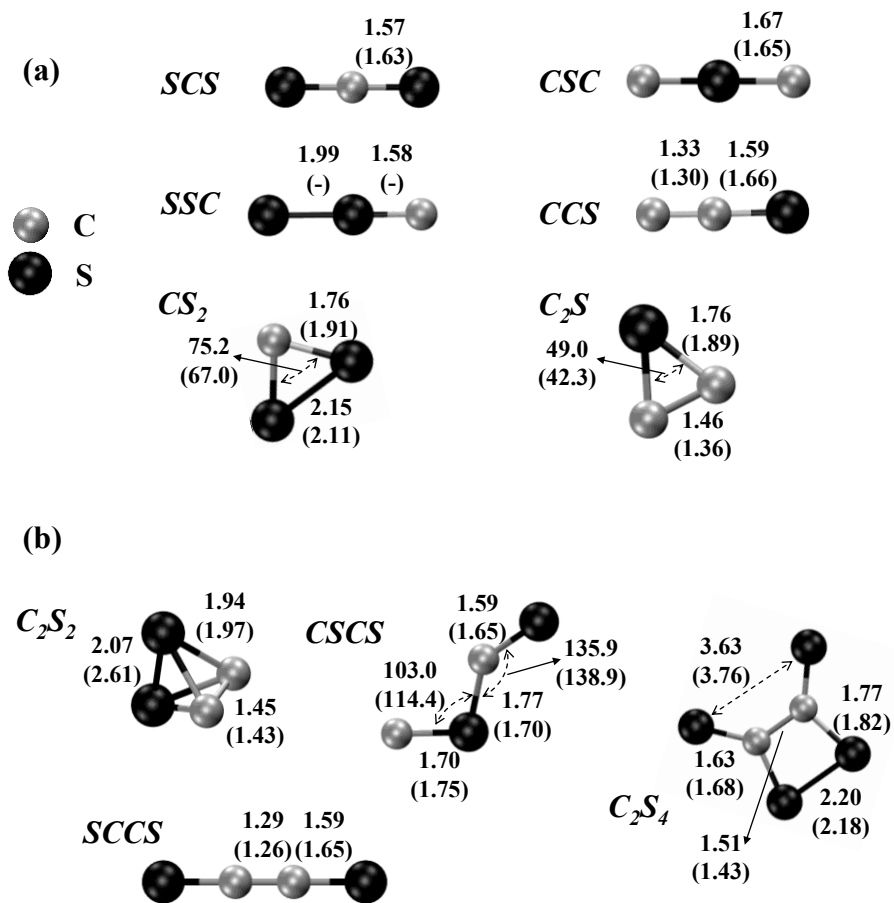


Figure 1.

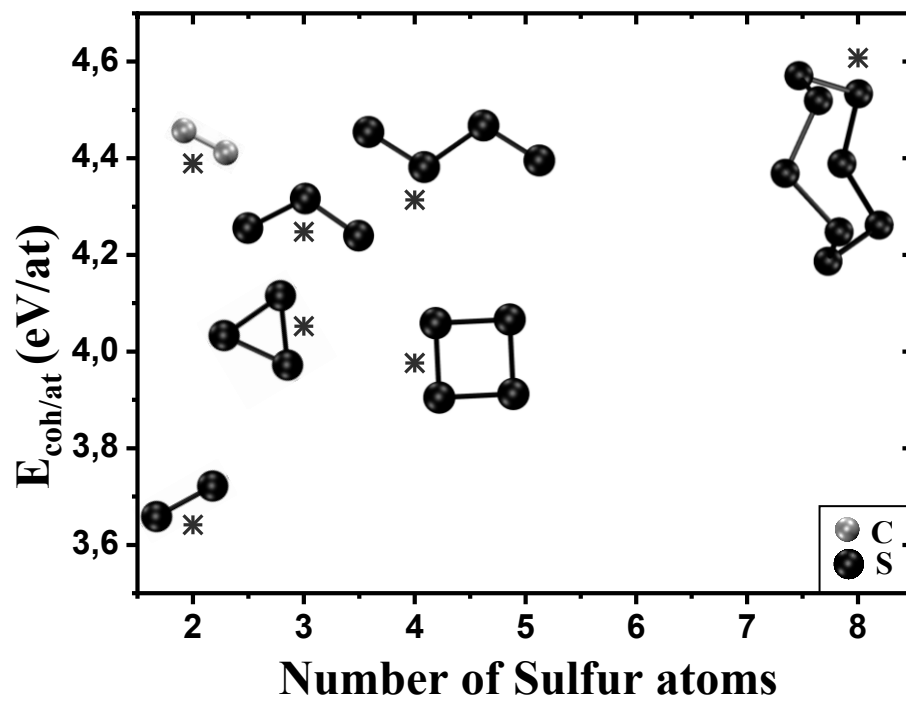


Figure 2.

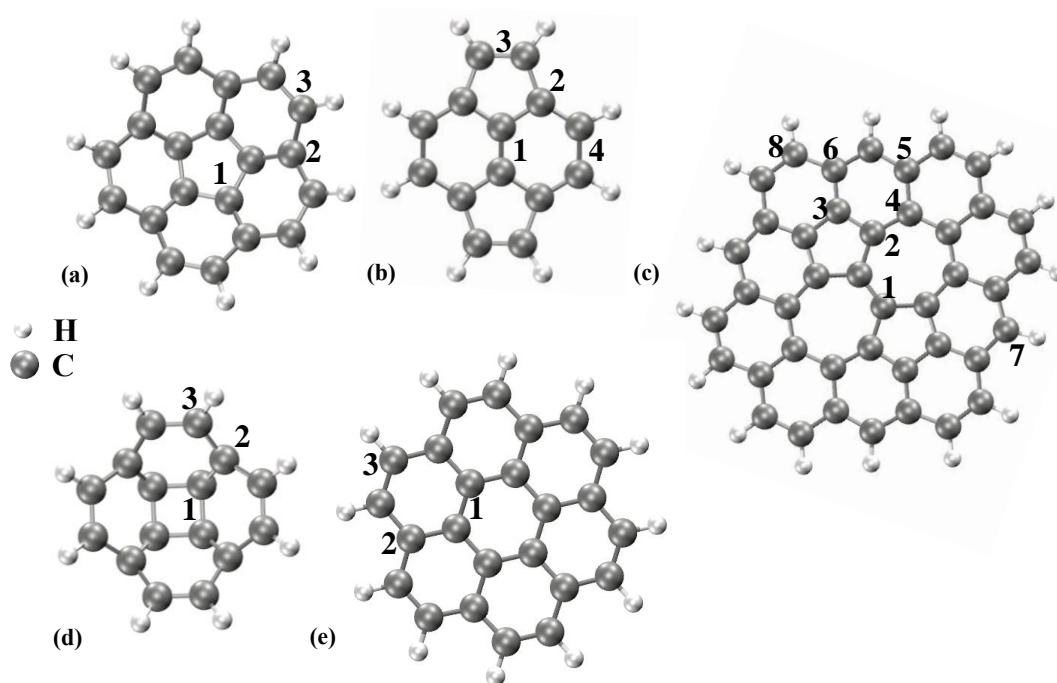


Figure 3.

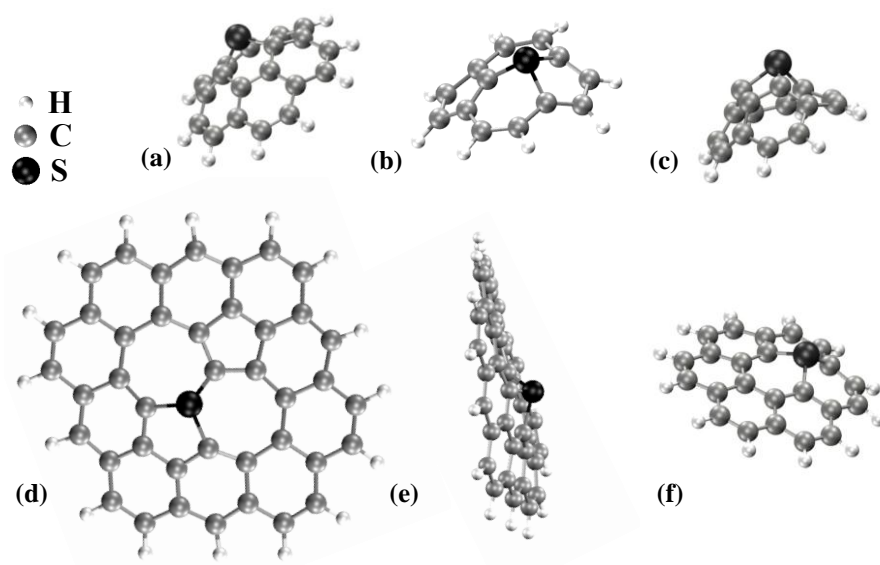


Figure 4.